J Mater Sci: Mater Med (2008) 19:75–81
DOI 10.1007/s10856-007-3107-5

Fabrication and characterization of needle-like nano-HA and HA/MWNT composites

Y. H. Meng · Chak Yin Tang · Chi Pong Tsui · Da Zhu Chen

Received: 12 October 2005 / Accepted: 14 June 2006 / Published online: 19 June 2007

Abstract Hydroxyapatite (HA) ceramic has been used in tissue engineering and orthopedics for its good biocompatibility and osteoconductivity. However, its clinical applications are usually limited by the low strength and brittleness. The objective of this research was to develop a new kind of HA composites in which multi-wall carbon nanotubes (MWNTs) were introduced to the HA ceramic matrix to improve the mechanical properties of the resulting composites. A simple chemical wet method was applied to synthesize the HA ceramic particles with the aid of surfactant and ultrasonication technique at normal atmospheric pressure. The morphology and microstructure of the synthesized HA were characterized by XRD and TEM as a function of treatment time. The results showed that the synthesized HA particles are needle-like with a length of 80–160 nm along the (211) direction and an aspect ratio of 5–15. MWNTs were treated with a mixture of nitric acid and sulfuric acid. The HA/MWNT composites were prepared by solution blending. The composites were sintered using a hot-press method. The mechanical properties of the HA/MWNT composites with different volume percentages of MWNTs were examined. The fracture toughness and flexural strength were improved by 50% and 28% separately when the volume percentage of MWNTs reached 7%.

Y. H. Meng · C. Y. Tang · C. P. Tsui (✉) · D. Z. Chen
Department of Industrial and Systems Engineering, The Hong Kong Polytechnic University, Hung Hom, Kowloon, Hong Kong, China
e-mail: mfgary@inet.polyu.edu.hk

Introduction

The hydroxyapatite (HA), as the main mineral constituent of human and animal hard tissues, has been considered as one of the most important substitute materials for bones and teeth [1–4]. Owing to its high biocompatibility and bioactivity, HA particles have been used to fill the bone defects in clinic [1] and used as bone cements [5, 6]. A strong chemical bond can be formed between the HA and the bone without forming a collagen interface layer after implantation [1, 7]. HA can also be used as a drug agent for its good biocompatibility and biodegradability [8]. Moreover, it has been used as reinforcing phase in some biocomposites [9–11].

Since nanotechnology arose in 1990s, synthesis and application of nano-sized hydroxyapatite (nano-HA) particles have been the focus of considerable research. Better mechanical strength can be achieved for nano-ceramics as compared with conventional ceramics. Webster et al. [12] reported that osteoblast proliferation on the nano-HA was faster than that on conventional HA and the activity of osteoclast on the nano-HA was greater than that on the conventional HA [13]. In extracellular culture, the synthesis of alkaline phosphatase by osteoblast on nano-HA ceramics was faster than that on the conventional HA ceramics. This means that nano-HA has better osteointegrative property. It has been known that the apatite in human bones exists in the form of needle-like crystals dispersed in the collagen networks. Therefore, the HA with a special shape and in a nano-size similar to natural bone can be expected to produce biocomposites with better biocompatibility. Many methods, such as solid-state reaction [14], hydrothermal method [15], sol–gel method [7, 16], spark plasma method [17], spray dry method [18] and combustion method [19], have been developed to prepare

HA particles. However, most of these methods cannot obtain HA particles with similar morphology and crystallinity to HA in nature bone. The uniformity of the particle shape and size can influence the properties of ceramics after sintering [20]. In this work, the method of chemical co-precipitation was used to prepare needle-like HA in a nano-size. The suitable experimental conditions, including pH value, concentration of the starting chemicals, synthesis temperature and blending speed, were controlled precisely. Surfactant was added in the raw materials to improve the congregating property and control the morphology of HA particles.

The poor strength and fatigue failure limit the application of HA to the low or non-load bearing situations. In order to make good use of the bio-properties of HA and extend the scope of application of HA, second reinforcing phases are often added into the HA ceramics to improve their mechanical properties in addition to controlling the phase transformation and the growth of the grain size in sintering process. Some materials with high bioactivity and biocompatibility have been introduced into HA matrix, such as hydroxyapatite whisker (HAw) and bioglass. The addition of these materials can improve the bioactivity and biocompatibility of HA ceramics. However, the mechanical strength can only be improved a little and is not high enough for high load-bearing implants [3, 21]. Some bio-inert particles, such as Al_2O_3 and ZrO_2, have also been introduced in HA matrix [22–24]. The fracture toughness of this kind of ceramics is in the range of 1.4 Mpa $m^{1/2}$ to 2.5 Mpa $m^{1/2}$. However, the reliability is not stable for the generation of tiny cracks in the matrix and the bioactivity decrease with the increase of the volume percentage of inert phases. Therefore, it is essential to develop a new kind of HA ceramics without sacrificing the mechanical properties and bio-properties of HA ceramics.

Multi-wall carbon nanotubes (MWNTs) have been widely investigated in recent years due to their excellent mechanical properties. MWNTs also have good electrical and magnetic properties. This makes composites with MWNTs have good mechanical, magnetic and wave absorbing properties [25]. The influence of carbon fiber diameter on the activity of osteoblasts in long term has been studied by Elias et al. [26]. The results showed that more osteoblasts proliferated on nano-diameter carbon fibers than on micro-diameter ones. More alkaline phosphatase can be synthesized by the osteoblasts on the carbon fibers with smaller diameters. Moreover, osteoblasts adhere more tightly to the nano-diameter carbon tubes than other implant materials [27]. The results indicate that carbon nanotubes have good bone integrative and conductive properties. All these properties have endowed the carbon nanotubes the predominance to be used as a reinforcing phase in biocomposites. In this study, the needle-like nano-HA particles were synthesized with the aid of surfactant and ultrasonication technique under normal atmospheric pressure, and HA/MWNT composites were produced by solution blending with high quality. The component, morphology and microstructure of the synthesized nano-HA were characterized by X-Ray Diffraction (XRD) and Transmission Electron Microscope (TEM). The structural and mechanical properties of the HA/MWNT composites were also determined.

Experimental

Fabrication of HA and HA/MWNT composites

For the synthesis of hydroxyapatite, calcium nitrate $Ca(NO_3)_2 \cdot 4H_2O$ (Analytical Reagent) and ammonium phosphate $(NH_4)_2HPO_4$ (Analytical Reagent) were used as the source materials. Cetyl trimethyl ammonium bromide (Chemical pure) was chosen as the surfactant. Firstly, $Ca(NO_3)_2 \cdot 4H_2O$ and $(NH_4)_2HPO_4$ were separately dissolved in deionized water to form solutions at the same concentration of 0.25 mol/L with pH values of 10.4 and 10.6. The volume ratio of the two solutions was 10:6. Secondly, cetyl trimethyl ammonium bromide was added into the $Ca(NO_3)_2$ aqueous solution. Thirdly, the solution of $(NH_4)_2HPO_4$ was dropped slowly to the former solution under vigorous stirring to get a homogeneous solution. The resulting solution was heated from 45 °C to 90 °C in a water bath for 1 h. After that, ultrasonic vibration at a frequency of 47 kHz and an output power of 158 W was used to promote the nucleation and the formation of fine HA crystals. The pH value of the solution was kept at 10.5 in the reacting process. A series of HA particles at three different treatment time (30, 60 and 120 min) have been synthesized. The precipitates obtained were centrifugated and rinsed with water and alcohol for several times, and then dried in a vacuum oven at 50 °C for 12 h. Some of the synthesized HA particles were calcinated at 900 °C for 30 min.

MWNTs supplied by Shenzhen Nano Tube Port Limited, P.R. China were used to reinforce the HA ceramic. The diameters of MWNTs are less than 10 nm while their length are 5~15 μm. The HA/MWNT composites with different volume percentages of MWNTs (2.4, 6, 7, 11 and 25%) were prepared by solution blending method. Owing to the chemical ''inert'' and the highly hydrophobic property of the MWNTs surface, it is required to modify the surfaces of the MWNTs to ensure the efficient tube–matrix interaction. Moreover, commercially available MWNTs usually have large surface energy and aggregate seriously. If the MWNTs cannot be dispersed evenly in the HA ceramic matrix, the strength of HA/MWNT composites

may decrease rapidly. In order to solve this problem, MWNTs were treated by a mixture of nitric acid and sulphuric acid at 120 °C for 20 min in this study. The surface-treated MWNTs and synthesized HA particles were mixed in an aqueous solution under vigorous stirring for 4 h to obtain the HA/MWNT composite.

Sintering process

After filtrating and drying, the HA/MWNT composite was sintered using a hot-press method in a graphite die with a diameter of 20 mm. The thickness of the specimens is 3.5 mm. High sintering temperature is good for densification of ceramics. However, it has been reported that HA began to decompose to α-$Ca_2P_2O_7$ and γ-$Ca_3(PO_4)_2$ with a growth in its grain size if the sintering temperature was higher than 1,200 °C [28, 29]. There was no dehydroxylation process during the hot-press sintering process of HA [30]. The composite powder was sintered at 1,200 °C for 30 min with pressure of 28 MPa in an atmosphere of nitrogen.

Characterization

The synthesized particles were characterized by X-Ray diffraction (XRD; Bruker D8 Advanced, Germany) with CuK_α (λ = 0.15418 nm) incident radiation. The accelerating voltage and current were 40 kV and 40 mA, respectively. The scan rate was 2°/min with a step size of 0.02°. Transmission Electron Microscope (TEM; H800, Japan) was used to study the morphology of the HA particles. The samples were dissolved in ethanol under ultrasonic vibration for half an hour before TEM examination. The fractured surfaces of HA/MWNT composites were observed using a scanning electron microscope (SEM, Leica Stereoscan 440, UK). The surface of the specimen was coated with a thin layer of gold prior to the SEM examination.

Mechanical testing

The flexural strength and fracture toughness of the HA/MWNT composite were determined in this study. All the testing samples (width = 4 mm; thickness = 3 mm; length = 36 mm) were cut using an automatic inner-circle slice machine, and then grinded and polished. The flexural strength of the composite was determined in electronic universal testing machine (WD-10, China). The span used was 30 mm, and the loading speed was 5 mm/min. Indentation fracture method [31, 32] was used to determine the fracture toughness of the composite. The indentations were made in a Micro Hardness Tester (Type M, Shimadzu, Japan). A load, P of 9.8 N was applied onto the sample surface, resulting in an indentation mark as shown in Fig. 1. The length of induced cracks, c was measured using an optical microscope (Leica Mikroskopie, Germany). The fracture toughness was then calculated from Eq. 1.

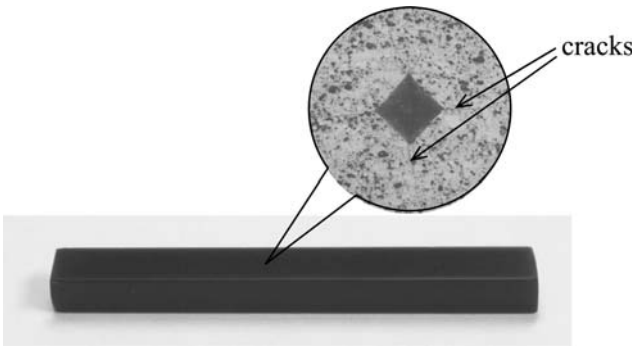

Fig. 1 The sample picture and indentation shape

$$K_{IC} = 0.0725Pc^{-\frac{3}{2}} \quad (1)$$

Experimental results

Characterization of synthesized HA particles

Figure 2 shows the TEM pictures of the synthesized HA obtained at different periods of heat-treatment time. The ultrasonic vibration can provide the energy for nucleation of the HA crystals and make the particles have high surface energy, resulting in promotion of the crystal growth along the (211) direction. After being treated for 30 min, the nano-sized HA in needle shape was obtained as shown in Fig. 2a. By increasing treatment time, the size of the crystals grows slowly as shown in Fig. 2b and c. From Fig. 2, it can be seen clearly that the synthesized HA particles were needle-like structure. The HA crystals in both human bones and teeth are needle-like and have the radius of 5~20 nm and the length of 60~100 nm [33], so the synthesized HA particles are similar to the natural ones.

Figure 3a shows the XRD pattern of the synthesized HA. The diffraction peaks, 2θ can be determined by comparing the XRD patterns with JCPDS file (No. 9-432). In this figure, the crystalline peaks at 25.9°, 31.8°, 32.0°, 33.0° and 40.0° exhibit a structure of monophase crystals of HA. Peaks at 25.9° and 31.8° represent (002) and (211) directions of crystals, respectively. The intensity ratio of these two peaks is about 1.0:2.1, indicating that HA crystals grow preferentially along C axis under the influence of surfactant and ultrasonic vibration. After calcination at 900 °C, the HA particles have the diffraction peaks shown in Fig. 3b sharper than those without calcination as illustrated in Fig. 3a. This indicates that the HA particles without calcination are of weak crystallinity similar to those in human bones. The XRD results also show that the

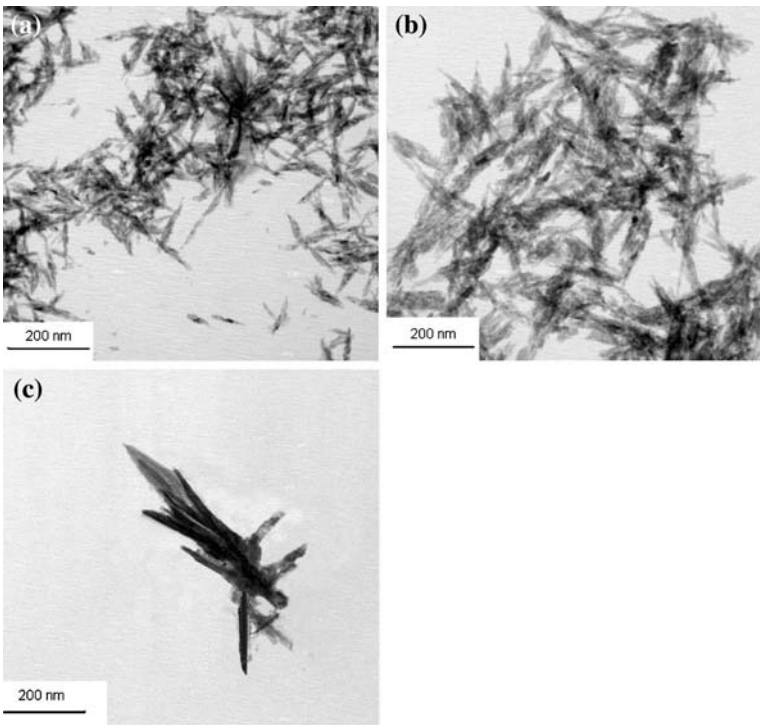

Fig. 2 TEM images of the synthesized HA obtained at different periods of heat-treatment time, t (**a**) t = 30 min, (**b**) t = 60 min, (**c**) t = 120 min

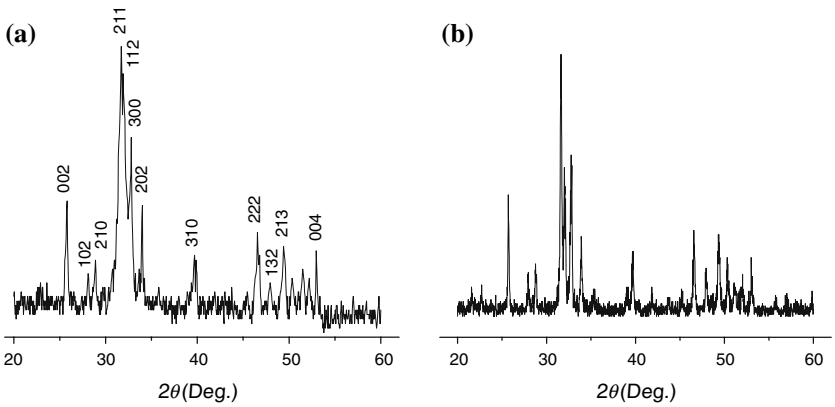

Fig. 3 XRD patterns of the synthesized HA particles (**a**) No treatment by calcinations. (**b**) With calcination at 900 °C

synthesized HA is stable. There is no decomposition after calcination at 900 °C.

Properties of HA/MWNT composite

XRD pattern of HA/MWNT composite

The XRD pattern of sintered HA/MWNT composite with 7 vol% of MWNTs shown in Fig. 4 shows that the main composition in the composite is HA. It is because there exists the crystalline peaks at 25.9°, 31.8°, 32.0°, 33.0° and 40.0°, which constitute the structure of monophase HA crystals. The presence of MWNTs can be characterized by the diffraction peak at 26.5°. There are no peaks of $Ca_2P_2O_7$ and $Ca_3(PO_4)_2$ indicating that there is no decomposition of HA after sintering.

Fracture toughness and bending strength of HA/MWNT composites

The fracture toughness and the flexural strength of the HA/MWNT composites with respect to the volume percentage of MWNTs plotted in Fig. 5. At low loadings of MWNTs, the fracture toughness and flexural strength increase with increasing volume percentage of MWNTs. The fracture toughness and flexural strength could be improved by 50% and 28%, respectively at 7 vol% of MWNTs. However, when the volume percentage of MWNTs is higher than 7%,

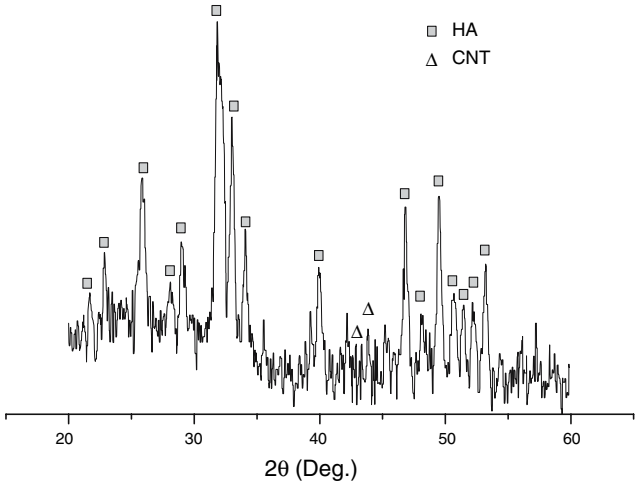

Fig. 4 The XRD pattern of the sintered HA/MWNT composite with 7 vol% of MWNTs

both the fracture toughness and the flexural strength of the composites decrease with the increasing of the MWNTs loadings.

Discussion

MWNTs dispersed in the HA matrix can absorb some fracture energy and prevent propagation of cracks. There are three main toughening mechanisms for MWNTs in the HA matrix: creak deflection, bridging and pull-out of MWNTs. When the cracks propagate and reach the MWNTs, they will deflect and propagate along the interface between the HA and MWNTs. The deflected crack can absorb more fracture energy. As shown in Fig. 6, MWNTs can also bridge the gap of the crack and prevent the crack propagating further, resulting in increase of the strength and toughness. Figure 7 shows the pull-out of MWNTs from the matrix. The interfacial adhesion and interfacial sliding behavior between HA and MWNTs can influence the strengthening and toughness effect of MWNTs. Moreover, high binding strength between HA and MWNTs can absorb high fracture energy. In this work, MWNTs

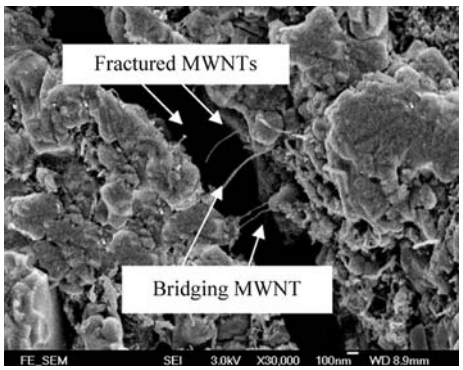

Fig. 6 SEM image of the crack in HA/MWNT composite

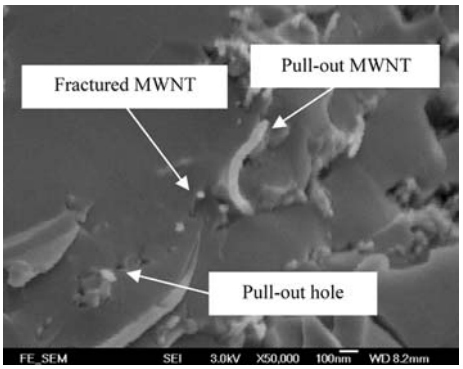

Fig. 7 SEM image of the fracture surface of HA/MWNT composite

were treated in a mixture of nitric acid and sulphuric acid. Many –COOH groups can be generated on the MWNTs surfaces after treatment. Therefore, chemical bonding between the functional group of MWNTs and cations of the HA particles can be generated, such as –COO–Ca–OOC– [34]. This improves the bonding strength between HA and MWNTs, hence enhancing the strength and toughness of the composites.

The SEM images of the sample fracture surfaces shown in Fig. 8 reveal that MWNTs still exist after sintering, even though the volume percentage of MWNTs decrease at a certain extent due to the their decomposition at high temperature. MWNTs have been dispersed homogeneously in

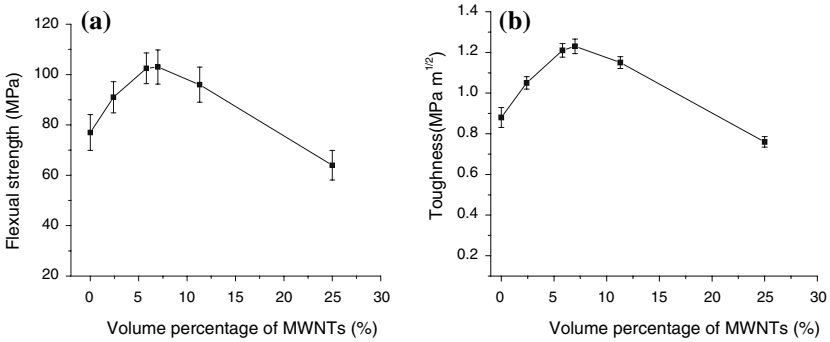

Fig. 5 The flexural strength (**a**) and the toughness (**b**) of the composites with different volume percentage of MWNTs

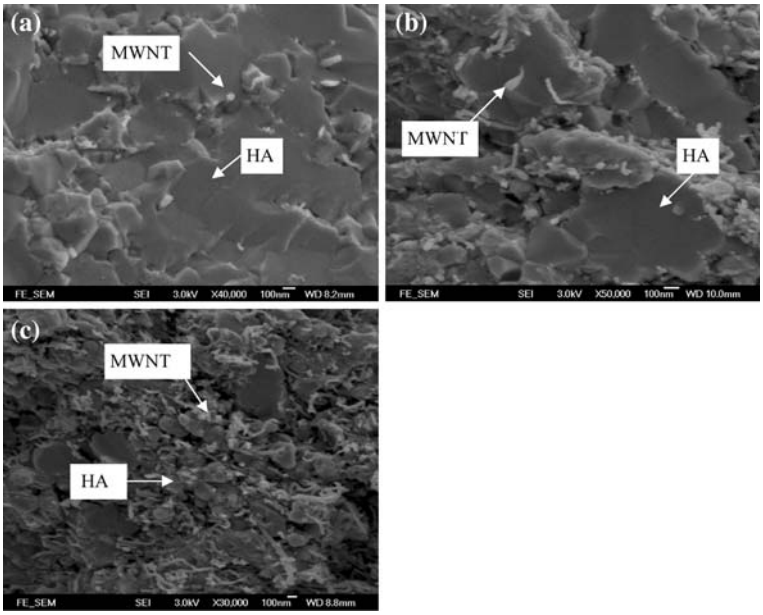

Fig. 8 The SEM images of the fracture surface of HA/MWNT composites with different volume percentage of MWNTs (**a**) 2.4 vol% (**b**) 7 vol% (**c**) 25 vol%

the HA matrix when the volume percentage of MWNTs is less than 7%. However, it can be observed from Fig. 8a that there are many aggregations of MWNTs when the volume percentage reaches 25%. It is because the chance of aggregation of MWNTs becomes larger with the increase in the volume percentage of MWNTs. The bonding energy of the interface between aggregated MWNTs is weak and there are generally pores between the aggregated MWNTs and the ceramic matrix. The aggregation and the pores become the defects in composite and weaken the matrix. This explains why the mechanical strength and toughness of HA/MWNT composite decrease when the volume percentage of MWNTs is higher than 7%.

Conclusion

Nano-sized and needle-like HA particles were synthesized with the aid of the surfactant and ultrasonic vibration. The surfactant could influence the shape of the HA crystals through electrostatic and co-ordination chemistry. It can be revealed from the SEM images that the dispersing properties of MWNTs after being treated by the nitric acid and sulphuric acid can be improved. The TEM images shows that the degree of crystallization of HA also increases with an increase in heat treatment time up to 120 min. The functional groups –COOH generated on the MWNTs surface after treatment are favorable for chemical bonding between the HA and MWNTs. With the incorporation of the MWNTs into the synthesized HA ceramic, the flexural strength and fracture toughness of the resulting HA/MWNT composites increase with the increase of volume percentage of MWNTs up to 7 vol%. This is attributable to the reason that the bridging, pull-out and fractured MWNTs as observed from the SEM images could reinforce the composite. However, with further increase in MWNTs over 7 vol%, the flexural strength and the fracture toughness of the composites decrease. It is because MWNTs aggregate at high volume percentage of MWNTs. The pores and weak bonding between aggregated MWNTs impair the flexural strength and the fracture toughness of the composite.

Acknowledgement The authors would like to thank for the support from the Research Committee of The Hong Kong Polytechnic University (Project code: RGU2). The authors wish to thank Prof. J.H. Zhang and Miss C.X. Liu for their assistance in sample preparation.

References

1. L. L. HENCH and J. WILSON, *An introduction to bioceramics*, (Singapore: World Scientific, 1993)
2. V. SHINY, P. RAMESH, M. C. SUNNY and H. K. VARMA, *Mater. Lett.* **46** (2000) 142
3. W. SUCHANEK, M. YOSHIMURA, M. KAKIHANA and M. YOSHIMURA, *Biomaterials* 17 (1996) 1715
4. M. BONNER, I. M. WARD, W. MCGREGOR, K. E. TANNER and W. BONFIELD, *J. Mater. Sci. Lett.* **20** (2001) 2049
5. T. N. OPARA, M. J. DALBY, E. J. HARPER, L. DI SILVIO and W. BONFIELD, *J. Mater. Sci.: Mater. Med.* **14** (2003) 277
6. E. J. HARPER, M. BRADEN and W. BONFIELD, *J. Mater. Sci.: Mater. Med.* **11** (2000) 491
7. S. R. RADIN and P. DUCHEYNE, *J. Biomed. Mater. Res.* **27** (1994) 35
8. D. M. LIU, T. TROCZYNSKI and W. J. TSENG, *Biomaterials* **22** (2001) 1721
9. J. P. FAN, C. P. TSUI, C. Y. TANG and C. L. CHOW, *Biomaterials* **25** (2004) 5363

10. J. P. FAN, C. P. TSUI and C. Y. TANG, *Mater. Sci. Eng. A* **382** (2004) 341
11. X. L. XIE, C. Y. TANG, K. Y. Y. CHAN, X. C. WU, C. P. TSUI and C. Y. CHEUNG, *Biomaterials* **24** (2003) 1889
12. T. J. WEBSTER, C. ERGUN, R. H. DOREMUS and R. W. SIEGEL, *Biomaterials* **21** (2000) 1803
13. T. J. WEBSTER, C. ERGUN, R. H. DOREMUS, R. W. SIEGEL and R. BIZIOS, *Biomaterials* **22** (2001) 1327
14. T. IKOMA and A. YAMAZAKI, *J. Solid State Chem*. **144** (1999) 272
15. F. ZHANG, Z. H. ZHOU, S. P. YANG, L. H. MAO, H. M. CHEN and X. B. YU, *Mater. Lett.* **59** (2005) 1422
16. G. BEAAI, G. CELOTTI, E. LANDI, T. M. G. LA TORRETTA, I. SOPYAN and A. TAMPIERI, *Mater. Chem. Phys*. **78** (2003) 816
17. M. OMORI, T. ONOKI, T. HASHIDA, A. OKUBO and Y. MURAKAMI, *Ceram. Int.* **1** (2005) 1
18. P. LUO and T. G. NIEH, *Mater. Sci. Eng.* **C3** (1995) 75
19. A. CUNEYT TAS, *J. Eur. Ceram. Soc.* **20** (2000) 2389
20. K. KENDALL, *Powder Technol.* **58** (1989) 151
21. C. K. WANG, C. P. JU and J. H. CHERN LIN, *Mater. Chem. Phy.* **53** (1998) 138
22. H. X. JI and P. M. MARQUIS, *Biomaterials* **13** (1992) 744
23. H. JI and P. M. MARQUIS, *J. Mater. Sci.* **28** (1993) 1941
24. A. RAPACZ-KMITA, A. SLOSARCZYK and Z. PASZKIEWICZ, *J. Eur. Ceram. Soc.* **1** (2005) 1
25. S. IIJIMA, *Nature* **354** (1991) 56
26. K. L. ELIAS, R. L. PRICE and T. J. WEBSTER, *Biomaterials* **23** (2002) 3279
27. R. L. PRICE, M. C. WAID, K. M. HABERSTROH and T. J. WEBSTER, *Biomaterials* **24** (2003) 1877
28. T. K. ANEE, M. ASHOK, M. PALANICHAMY and S. N. KALKURA, *Mater. Chem. Phys.* **80** (2003) 725
29. S. RAYNAUD, E. CHAMPION, D. BERNACHE-ASSOLLANT and P. THOMAS, *Biomaterials* **23** (2002) 1065
30. A. RAPACZ-KMITA, C. PALUSZKIEWICZ, A. SLOSARCZYK and Z. PASZKIEWICZ, *J. Mol. Struct.* **744–747** (2005) 653
31. K. TANAKA, *J. Mater. Sci.* **22** (1987) 1501
32. Z. LI, A. GHOSH, A. S. KOBAYASHI and R. C. BRADT, *J. Am. Ceram. Soc.* **72** (1989) 904
33. Y. B. BAO, C. P. A. T. KLEIN, X. D. ZHANG, K. de GROOT and Y. B. KLEIN, *Biomaterials* **5** (1994) 835
34. H. L. DAI, X. Y. WANG, J. HUANG, Y. H. YAN and S. P. LI, *Trans. Nonferrous Met. Soc. China* **14** (2004) 769